AIAA Propulsion and Energy Forum
19-22 August 2019, Indianapolis, IN
AIAA Propulsion and Energy 2019 Forum

10.2514/6.2019-3900

Experimental Investigation of Mixtures of 1-Ethyl-3-Methylimidazolium Ethyl sulfate and Ethylammonium Nitrate with Electrospray Propulsion Applications

Mitchell J. Wainwright,[1]
Missouri University of Science and Technology, Rolla, Missouri, 65409
Joshua L. Rovey,[2]
University of Illinois Urbana-Champaign, Urbana IL, 61801
Shawn W. Miller,[3]
Boston College, Institute for Scientific Research, Chestnut Hill, MA, 02467
and
Benjamin D. Prince,[4]
Air Force Research Laboratory, Space Vehicle Directorate, Kirtland AFB, NM, 87117

Physical properties, performance metrics, and mass spectra of mixtures of two ionic liquids (1-ethyl-3-methylimidazolium ethyl-sulfate aka [Emim][$EtSO_4$] and ethylammonium nitrate aka EAN) are investigated from the standpoint of electrospray propulsive characteristics. Spectra suggest that as the [Emim][$EtSO_4$] mixture fraction increases, the intensity of [Emim][$EtSO_4$] related species in the plume also increases, while the presence of EAN decreases. Spectra also show presence of both EAN proton transfer species and species related to chemical reaction of [$EtSO_4$] and water. Despite the volatility of EAN, it emits stably into vacuum at low flow rates when mixed with 25% [Emim][$EtSO_4$]. Spectra also show species swapping between [Emim][$EtSO_4$] and EAN, suggesting microscopic reorganization and non-linear mixing of physical properties. Experimental measurements of surface tension, conductivity, and density for various mixture mass percentages also show non-linear mixing characteristics. Conductivity differs by over 40% from linear predicted values. Analytic predictions of propulsion performance are presented based on the non-linear experimental property results, and compared to predictions based on linear mixing models. Results indicate non-linear mixing is important when making performance predictions, with differences of at least 40% possible. Curve fits of experimentally determined properties of the mixtures versus mixture ratio can be used to determine maximum or minimum performances based on different performance metrics (current, thrust, and specific impulse); for these ionic liquids the metrics are shown to optimize at different mixture mass percentages, over a 2% range; this range will increase when mixing liquids with more disparate densities.

Nomenclature

F	=	propulsive force (Thrust)
$f(\varepsilon)$	=	slope function of current vs. non-dimensional flow rate based on dielectric constant
g_0	=	acceleration due to gravity on Earth
K	=	conductivity
I	=	current emitted from electrospray source
I_{sp}	=	specific impulse

[1] Graduate Research Assistant, Department of Mechanical and Aerospace Engineering Missouri University of Science and Technology, Rolla, Mo, 65409, and Student AIAA Member. mjwmv4@mst.edu
[2] Associate Professor, Department of Aerospace Engineering, 317 Talbot Laboratory, 104 South Wright St., AIAA Associate Fellow.
[3] Research Engineer, Institute for Scientific Research, St Clement's Hall 402, 140 Commonwealth Ave, and Member AIAA.
[4] Research Chemist, Space Vehicles Directorate, 3550 Aberdeen Building 570 and Member AIAA

$\dot{m}$ = mass flow rate of propellant
n = degree of solvation
Q = volumetric flow rate
V_{acc} = accelerating voltage
γ = surface tension
ε = dielectric constant
ρ = density

I. Introduction

Ionic liquids (ILs) and mixtures of ILs are of broad interest in chemistry and in other areas of study, with a wide range of actual and potential applications [1]. Ionic liquids are molten salts with low melting temperatures; melting temperatures can even be below room temperature for some ILs. There are two main subcategories of ionic liquids: Aprotic Ionic Liquids (AILs) and Protic Ionic Liquids (PILs) [2]. AILs generally do not form hydrogen bond networks and are discussed in [3]. PILs form a hydrogen bonding network via a hydrogen atom from one ion bonding to a strong electronegative atom from another ion. PILs are formed from a Brønsted acid and a Brønsted base; their key property is proton transfer from the acid to the base [2, 4]. Interest in mixtures of ILs has increased significantly in recent years due to the flexibility obtained by mixing and matching cations and anions within a liquid mixture (or even formulating mixtures with more than one cation and more than one anion). Such flexibility may lead to the creation of designer solvents [1].

ILs have many properties that make them specifically attractive as propellants for electrospray propulsion. ILs exist as molten monoclinic salts with both cations and anions regularly present in the liquid state. This provides two readily available ion sources for electric propulsion systems. The large number of available ions combined with an IL's ability to alternate between cation and anion extraction modes also make them attractive as propellants. Altering the extraction mode is advantageous because the spacecraft does not develop a floating potential and thus no beam neutralizer is required, unlike for Hall-effect thrusters [5, 6]. ILs also have favorable physical properties such as low melting point, high conductivity, and low, often negligible, vapor pressure; characteristics that are also favorable for spacecraft propellants [7-9]. Additionally, ionic liquids, mainly PILs, can be decomposed. For instance, EAN is known to contain sufficient oxygen for combustion without augmentation and, when mixed with sulfolane [$C_4H_8O_2S$], can function as an electrospray propellant with nominal efficiency of 75%, thrust between 28 and 1200 N, and corresponding specific impulse between 150 and 2000 seconds [10]. The ability to combust makes ILs potential candidates for use in a combined, or multimode, combined chemical and electric propulsion system [7, 11, 12].

The use of mixtures of ionic liquids as multimode or dual mode propellants provides ultimate utility and diversity within the context of small spacecraft propellant design [5, 12-15] and have been extensively studied in previous investigations. Donius showed that the performance of an integrated system could provide wide flexibility and that such a system would be more mass-efficient and could operate in a broader design envelope than two separate state-of-the-art systems, due to shared hardware and propellant reducing total mass [15]. Ideally, for a multimode system, both chemical and electric mode operation would be separately investigated and the mixture ratio would be then tuned to provide as optimal a propellant as possible for a given mission in which both modes are used. Previous work on the development of such a propellant for small satellite applications has focused on optimizing the mixture based on chemical mode performance [16] while finding a combination that could still operate, albeit non-optimally, in the electric mode [6, 11, 12, 14]. No study to date has focused on the design and analysis of mixtures of ionic liquids from the standpoint of electrical mode applications. Tuning mixtures of these liquids to make them optimal for electric propulsion represents a significant challenge due to non-linear mixing behavior and the very large number of known anions and cations for ILs, i.e., critical mixture properties scale non-linearly with a linear combination of constituents. Further, there are a large number of cations and anions to choose from when formulating (designing) a mixture [1]. The focus of the current work is therefore to examine and analyze electrospray performance versus mixture ratios for two selected ILs and to contrast this performance with that obtained by utilizing simple linear mixing laws. This is done by 1) experimentally measuring the physical properties of various mixtures of two specific ionic liquids, 2) analyzing the theoretical performance of these mixtures as propellants using the experimentally obtained properties, and 3) experimentally obtaining mass spectra for the mixtures and relating the spectra to performance characterization.

Mass spectra such as has been obtained in the current study can offer insight into the chemical structure of liquids and the emission profile that liquids exhibit when electrosprayed [6, 7, 9, 17]. For instance, spectra results can identify specific ions that are present within a liquid mixture as well as provide information regarding ion

interactions, with one such interaction being ions from one IL pair with either neutrals or ions from the other IL. Such information can be useful in explaining the deviations in actual macroscopic properties and performance from that obtained using ideal mixing laws [1] and/or uncover deficiencies in currently implemented numerical models due to unanticipated and thus omitted species. Obtaining such results to compare models with has previously been highlighted as of interest [3]. The current study thus provides and relates both macroscopic results (property and performance information) and microscopic results (spectra information) regarding the aggregated effects that mixing ionic liquids have on propellant design.

Mixtures of two specific ionic liquids currently of interest to the multimode community are examined in this work; these ILs are ethylammonium nitrate (EAN) and 1-ethyl-3-methylimidazolium ethyl sulfate ([Emim][$EtSO_4$]). The former IL is a PIL and the second IL is an AIL. Specifics of these choices will be discussed more fully in the following section. Five total mixture ratios were chosen in order to provide sufficient experimental data to adequately assess the non-linear-variation in the physical properties of the mixtures, as well as to contrast performance predicted based on actual physical properties of the mixtures with performance based on typical linear mixing laws. The spectra for different mixture ratios are also experimentally obtained. The spectra results provide significant insight into the characteristics and interactions within the mixtures by showing the changes in intermolecular interactions by showing changes in emitted species with mixture mass percentage.

II. Ionic Liquid Selection

This section discusses the rationale for the selection of the two specific ionic liquids that are utilized in this study. Information on the PIL EAN will be presented first followed by information on the AIL [Emim][$EtSO_4$].

Ethylammonium nitrate (EAN), a PIL, is chosen because of its historic significance as well as current interest in it as a representative IL within the electrospray community [2]. The ability of the ethylammonium cation ([EA]) to delay ion evaporation and therefore "produce the smallest possible nano-drops, minimally polluted by ions" [10] is attractive. Additionally it is reactive [18]. The anion for EAN is nitrate ([NO_3]), a common anion in similar studies investigating mass spectra of ionic liquid propellants [6, 9]. EAN was potentially the first room temperature ionic liquid (RTIL), a category of ILs that exists in liquid form at room temperature [2]. This attribute makes storage on board spacecraft easier, since a lower melting temperature reduces the heating requirements for maintaining the propellant in liquid form [15]. EAN can be modeled in MD simulations [19]. Effects of surface sputtering of Si, SiC, Ge, and GaAs when electrospraying EAN have been observed; difficulty in electrospraying it as a neat, i.e. pure, IL at low flow rates in anion mode is also reported [20]. Additionally, there is evidence in the literature that both cations and anions of EAN are likely to undergo proton donor/receptor behavior, [9, 21, 22] that EAN will strongly alter the network within a mixture of ILs, and that the spectra of EAN mixed with another IL will be beneficial in terms of providing information desired by the modeling community [3, 23, 24]. Specifically, Alavi and Thompson found the barrier to proton transfer for both EAN and hydroxylammonium nitrate (HAN) to be at 3.7 and 13.6 kcal/mol, respectively [25, 26], and proton transfer in HAN has already been observed in electrospray spectra [6]. For EAN, this would result in the [EA] cation having one hydrogen atom proton transferring to the [NO_3] anion forming ethylamine [EA-H] and nitric acid [HNO_3]. The electrostatic interaction energies presented by [26] seem to suggest that neat EAN may be electrostatically energetically favorable over the proton transferred form. Further, even if a small amount of water is present in the mixture, the proton transfer is still likely to occur, as water aids proton transfer [27] and causes liquid restructuring [28].

1-ethyl-3-methylimidazolium ethyl sulfate ([Emim][$EtSO_4$]) is chosen as it has been extensively studied as a potential propellant component for a multimode system in conjunction with HAN [12-14, 29]. HAN exists as a solid monoclinic salt at room temperature and is thus not favorable for a mixture variation investigation such as this [6]. Thus the current choice also represents a pairing of one AIL ([Emim][$EtSO_4$]) and one PIL (EAN) that are both present in liquid form at room temperature. Experimental determination of properties for similar AIL and PIL pairing has been highlighted as of interest to the broader community [3]. [Emim][$EtSO_4$] potentials are also readily available for molecular dynamic modeling [30]. Therefore, both of these liquids and their mixtures can be modeled using molecular dynamics. Results obtained in the current study may therefore be used to provide validation for such models. In this study, the physical properties and plume characteristics of 0, 25, 50, 75, and 100% [Emim][$EtSO_4$] mixed with 100, 75, 50, 25, and 0% EAN by mass, respectively, are measured experimentally.

III. Experimental Procedure

This section describes the procurement and synthesis of the ionic liquids. The methodology and procedures used to obtain the experimental results in this study are also provided.

A. Propellant synthesis

For this study, the ionic liquids were procured, with characterized purity, from available sources, rather than synthesized. [Emim][$EtSO_4$] was obtained from Sigma Aldrich at a ≥ 95% purity level. EAN was obtained from Iolitec at > 97% purity. The removal of volatile impurities was conducted according to methodology previously developed and validated [6]. The presence of volatile impurities, specifically water, may lead to bubble formation during electrospray. The various mixture mass percentages were synthesized by extracting volatile impurities in vacuum for one day, as mass loss in the components, especially EAN was observed. Mixture mass percentage refers to the mass percentage of the total liquid composed of [Emim][$EtSO_4$]. These liquids were then mixed into batches with overall mass greater than 4 grams, according to the desired mixture mass percentages, to a precision within 0.01 g. Samples of neat and mixed ILs were exposed to high vacuum (10^{-7} Torr) before use in experimental measurements in order to boil off any volatile impurities which may have reconstituted from synthesis. Each sample was exposed separately to avoid cross contamination. Samples for mass spectra studies were left for over 12 hours in the mass spectrometer instrument [6] and those destined for physical property determination utilized a ~5 liter quartz vacuum chamber evacuated via a turbomolecular pump.

The chemical structure of both liquids investigated here are pictured in Fig. 1. The chemical formula for $[Emim]^+$ $[EtSO_4]^-$ is $[C_6H_{11}N_2]^+$ $[C_2H_5SO_4]^-$. EAN has two forms, one ionic, and the other a proton transferred form, both shown in Fig. 1. Therefore EAN has three charge-neutral species: 1) the neutral paring of the ethylammonium cation and nitrate anion: $[EA]^+$ $[NO_3]^-$, 2) the neutral proton donor ethylamine [EA-H], and 3) the neutral proton acceptor nitric acid [HNO_3]. Both ionic and proton-transferred versions of EAN are observed in subsequent discussions of mass spectra results; however, their exact concentrations in the liquid are unknown.

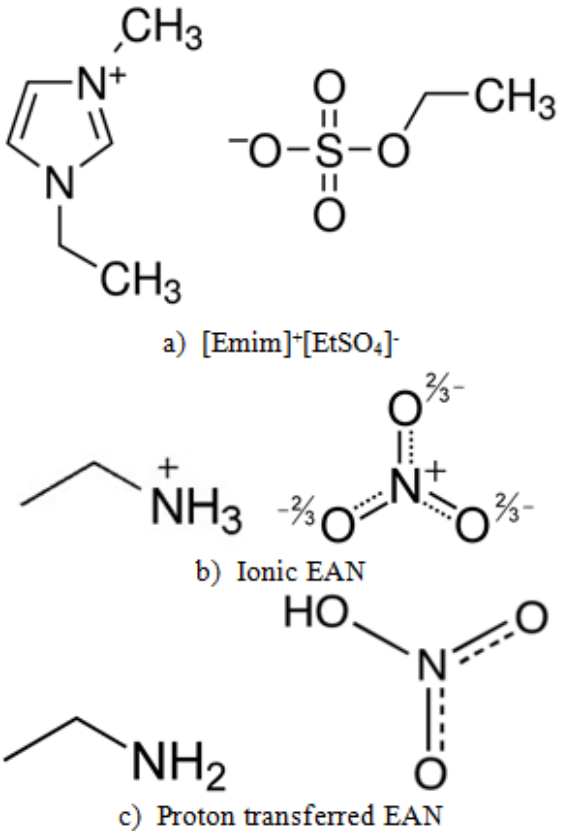

Fig. 1: Chemical structure of the constituents of the mixtures investigated here, $[Emim]^+$ $[EtSO_4]^-$ and both the ionic $[EA]^+$ $[NO_3]^-$ and proton-transferred (covalent) [EA-H][HNO_3] forms of EAN

B. Physical property measurements

Physical properties of conductivity, density, and surface tension for various mixture ratios of the ILs are measured. As stated previously, water content in samples was a concern; thus, before physical properties were

measured, the liquids were dried in a ~5 liter quartz vacuum chamber evacuated via turbo-molecular pump for greater than 1 hour.

The chemical structure of both liquids investigated here are pictured in Fig. 1. The chemical formula for $[Emim]^+$ $[EtSO_4]^-$ is $[C_6H_{11}N_2]^+$ $[C_2H_5SO_4]^-$. EAN has two forms, one ionic, and the other a proton transferred form, both shown in Fig. 1. Therefore EAN has three charge-neutral species: 1) the neutral paring of the ethylammonium cation and nitrate anion: $[EA]^+$ $[NO_3]^-$, 2) the neutral proton donor ethylamine [EA-H], and 3) the neutral proton acceptor nitric acid $[HNO_3]$. Both ionic and proton-transferred versions of EAN are observed in subsequent discussions of mass spectra results; however, their exact concentrations in the liquid are unknown.

C. Physical property measurements

Physical properties of conductivity, density, and surface tension for various mixture ratios of the ILs are measured. As stated previously, water content in samples was a concern; thus, before physical properties were measured, the liquids were dried in a ~5 liter quartz vacuum chamber evacuated via turbo-molecular pump for greater than 1 hour.

Conductivity was measured using an OAKTON Cond 6+ conductivity meter, accurate to +/- 1%. This instrument was calibrated immediately before measurements were acquired, using two different RICCA conductivity standards (7,000 µS/cm and 50,000 µS/cm, obtained from Cole Parmer), ensuring accuracy and precision over the full range of anticipated results. Conductivity measurements were made in accordance to the recommendations provided by the manufacturer by first thoroughly cleaning the probe, then rinsing it in the liquid of interest, and finally inserting the probe into the liquid; results were recorded after the reading stabilized.

Mass density was measured using a 2mL Pyrex specific-gravity bottle (pycnometer) obtained from Fischer Scientific. Pycnometers measure density by utilizing a well-known/well-characterized volume flask in conjunction with a scale to provide both mass and volume of the liquid. The volume of this vial was calibrated using distilled water at room temperature. All masses were measured using a Torbal AGC500 bench scale with an accuracy to 0.001 grams. This provides an overall uncertainty of 0.14% in density measurements, not including standard deviations in measuring the mass of the liquids of interest.

Surface tension was measured with a Ramé-Hart 500 Series Goniometer/Tensiometer instrument, with rated precision of 0.01 dynes/cm. The Ramé-Hart instrument utilizes a contour fitting algorithm to obtain the geometry of a liquid drop. This geometry and the numerical integration of the Young-Laplace equation provides a surface tension value. The methods employed matched that specified by the manufacturer.

D. Electrospray source and quadrupole mass spectrometer

The electrospray source and mass spectrometer are used in tandem to provide angularly resolved mass spectra. A schematic of both the quadrupole and the electrospray source is provided in Fig. 2. This setup has been extensively described in previous work [6-8, 17]. The source has a 50 µm inner diameter capillary (PicoTip MT320-50-5-5) with an extractor grid set approximately 1.5 mm downstream of the capillary emitter. This grid has a hole that is approximately 1.5 mm in diameter which blocks emissions at angles greater than approximately 30° off the centerline. Both emitter and extractor are mounted on a rotational stage that is attached to a custom made vacuum flange due to finite thickness of extractor. This flange provides feedthrough for high-voltage connections and propellant lines. Everything to the right of the vacuum feedthrough, shown in Fig. 2, is operated in high vacuum (at a nominal pressure of $1x10^{-7}$ Torr). The emitter capillary is connected to the propellant feed system through a 100-µm ID fused silica capillary. This fused silica capillary passes through the custom made vacuum feedthrough. The reservoir is a syringe situated on a Harvard Elite Module PicoPump. This syringe pump is external to vacuum and provides volumetric control at ± 2% over the range investigated. The syringe, capillary, and capillary emitter are replaced when the liquid under investigation is changed in order to avoid cross contamination. This experimental setup is essentially the same in function and principle as the pressure fed mode, this comparison is described fully in [31].

The experimental work discussed here uses an approximate 2.3 kV potential difference between the emitter and extractor. This is applied as a -0.5 kV bias on the emitter and a +1.8 kV bias on the extractor, with respect to facility ground, for the anion mode. Switching to the cation mode involves switching the electric field to 0.5 kV on the emitter and -1.8 kV on the extractor. This potential difference is similar to that used in previous work [6] and is in agreement with the value for the electric field that is expected based on theoretical means for determining starting voltage in electrospray and liquid metal ion sources [32]. Spectra were acquired in the 20 pL/sec to 3 nL/sec range at angles ranging from -45° to 45° in 5° increments for both cation and anion emission modes. EAN spectra was only taken for the flow rate of 3 nL/sec, as stable electrospray at lower flow rates was not able to be obtained. This difficulty has been observed and discussed before for anion emission [20]. Volatility has been cited as the reason for

EAN's failure to electrospray at low flow rates in vacuum [10, 33]. This effect is further confirmed by our own observation of boiling on the meniscus.

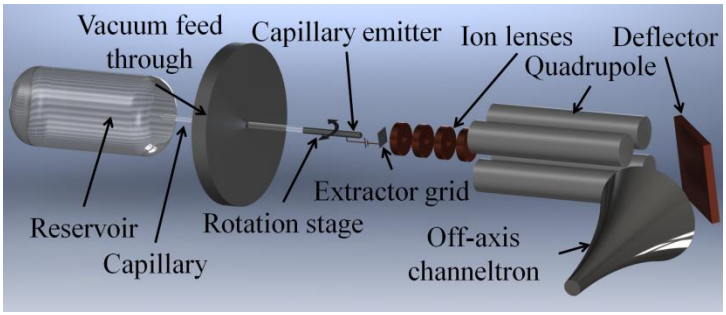

Fig. 2: Diagram of mass spectrometer experimental setup showing the reservoir, capillary, vacuum feed-through, capillary emitter, rotation stage, extraction grid, ion lenses, quadrupole mass filter, and off-axis channeltron detector

The spectra were obtained with a quadrupole mass spectrometer. This specific quadrupole mass spectrometer and its use has been described previously in the literature [8, 34]. In this device, the electrospray beam is emitted from the capillary emission source, through the extractor grid, and then through a series of ion lenses that focus the ion beam for maximum signal. The beam then enters the quadrupole where a specific mass-to-charge ratio (or sometimes referred to as m/q) is selected and allowed to pass; this study uses m/q rather than amu/q for brevity. Ions with other m/q values are rejected by de-stabilizing their trajectories. After the ions with selected m/q pass through the quadrupole, the particles are redirected into an off-axis channeltron single-channel electron multiplier for counting via a deflector. The channeltron registers a count every time a particle is detected. The counts at each m/q value are integrated for 100 ms. The mass step size of the quadrupole instrument was set to 1 m/q. Calibration experiments have shown agreement with expected species to within 2 m/q, and thus m/q peaks in these spectra are expected to be resolved to within 2-3 m/q. As ions with significant kinetic energy pass through the quadrupole, the resolution of spectra peaks can be degraded at low mass values; this "zero mass" can extent to large m/q values and is present as a baseline in the spectrum.

IV. Experimental Results

In this section, physical chemistry and mass spectra results for mixtures of the ionic liquids are presented, compared, and contrasted to previously reported results in the literature. General and specific implications and observations relevant to the design and application of mixtures of ionic liquids as electrospray propellants are reserved for the subsequent analysis and discussion section.

A. Volatility of liquids

As discussed in the Introduction, neat EAN is not readily electrosprayed at low flow rates due to the volatility of EAN. In contrast a composition of 25% [Emim][$EtSO_4$] and 75% EAN is found in this work to be electrosprayable at low flow rates. This is noteworthy as it suggests that the addition of [Emim][$EtSO_4$] stabilizes the volatility of EAN (see Fig. 3), and thus makes EAN sprayable in both cation and anion modes at 20 pL/sec (albeit in conjunction with addition of [Emim][$EtSO_4$]). This section presents quantitative results that suggest EAN is more volatile than the 25% [Emim][$EtSO_4$] and 75% EAN solution, suggesting [Emim][$EtSO_4$] stabilizes EAN's electrospray by reducing the rate at which the liquid evaporates.

In Fig. 3, the x-axis represents the mass percent of [Emim][$EtSO_4$] in the liquid and the y-axis represents the chamber base pressure after one hour of operation with the liquid inside the chamber. This chamber is the quartz chamber used for evaporating off any volatile impurities from the liquids before physical property data is obtained (i.e., it is not the chamber used for acquiring mass spectra). Fig. **3** shows a reduction in chamber base pressure with mixture mass percent of [Emim][$EtSO_4$]. This reduction in base pressure is believed to be due to a reduced volatility of the investigated liquid (sample ~20 g). This observed reduction in base pressure with increase in mixture mass percentage of [Emim][$EtSO_4$] supports the volatility hypothesis [10].

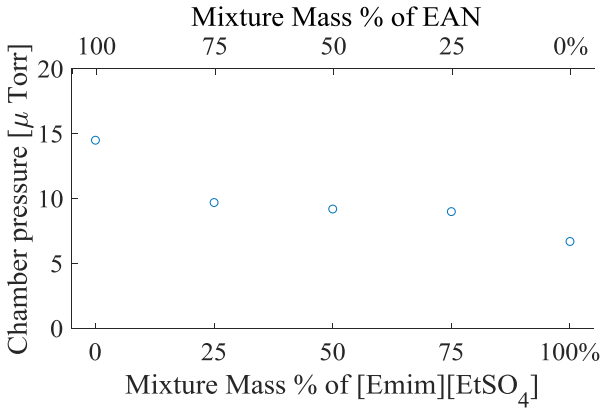

Fig. 3: Chamber base pressure after one hour for various mixture mass percentages.

Fig. 3 shows that the chamber base pressure exhibits non-linear behavior with respect to mixture mass percentage during vacuum drying of volatile components. The non-linear trend in chamber base pressure demonstrates that there is a corresponding non-linear effect on volatility, and thus evaporation. These non-linear changes could enable electrospray of volatile components by holding them in a non-volatile liquid in order to reduce volatility and thus stabilize cone jet extraction.

Based on Fig. 3 and the observed electrospray behavior of these liquids, it appears that electrospray emission of one (volatile) ionic liquid may be stabilized via the addition of a second (non-volatile) ionic liquid. Attempts to electrospray 97% pure EAN, for flow rate values at and below ~1 nL/sec did not result in stable and sustained emission, while the emission at 3 nL/sec was stable. This is may be due to EAN's volatility as discussed previously by Alonso-Martilla [10]. Evidence of a variation in volatility with mixture ratio is also observed (see Fig. 3) by the increase of 50% in facility pressure when a vial of neat EAN is in the vacuum chamber, compared to the pressure for a mixture of [Emim][EtSO$_4$] and EAN. When attempting to electrospray EAN, the quadrupole instrument had a base pressure of $3x10^{-6}$ Torr; however, when the syringe pump was set to zero flow rate (of EAN) this pressure reduced to $1x10^{-7}$ Torr, further supporting the volatility hypothesis. [Emim][EtSO$_4$] was readily emitted via electrospray from the 3 nL/sec flow rate down to the 10's of pL/sec. Lower flow rates were not investigated, as the focus here was not in finding the lowest flow rate but rather in characterizing liquid mixtures where a larger population of ion emission is expected. By mixing these two ILs together with a mass ratio of 25% [Emim][EtSO$_4$] and 75% EAN, stable emission was observed over the flow rate range of interest, this may be due to a change in the rate of evaporation as evidenced by Fig. 3.

B. Physical chemistry data

In this section, the experimentally obtained physical chemistry data for mixtures of the selected ionic liquids is presented. Specifically, values for conductivity, surface tension, and density are described for various mixture mass percentages of these liquids. These properties are critical for analyzing and determining performance in electrospray propulsion.

In Fig. 4, the x-axis represents the mixture mass percentage of [Emim][EtSO$_4$]. The y-axis represents density (ρ) in [g/cc], surface tension (γ) [dynes/cm], and conductivity (κ) [mS/cm] in Figures a), b), and c) respectively. Linear and polynomial curve fits of density, surface tension, and conductivity are also presented over the experimental values for comparison. The measured value of 1.240 g/cc for neat [Emim][EtSO$_4$] and 1.214 g/cc for neat EAN are <1% different from the values reported in previous work of 1.240 g/cc for [Emim][EtSO$_4$] and 1.212 g/cc for EAN [35, 36]. The surface tension measurements of 49.7 dynes/cm for neat [Emim][EtSO$_4$] also agrees with the value reported in previous literature of 47.25 dynes/cm [36]. In addition, the measured EAN value of 45.97 dynes/cm agrees well with the previously reported value of 47.3 dynes/cm for EAN [2], being 5% and 2% different, respectively). The conductivity value of 21.6 mS/cm is similar to the EAN literature values presented of 24.8 mS/cm (~13% difference) [3], and 26.9 to 45.0 mS/cm [2]. The large range may be due to proton transfer reducing the number of cations and anions, reducing the number of charge carriers, and thus reducing conductivity [37]. The value for [Emim][EtSO$_4$] of 3.41 mS/cm is larger than the 80 µS/cm reported in literature [36]. The discrepancy in the conductivity results for [Emim][EtSO$_4$] was investigated and the same result was obtained in repeated tests; additionally, the source of the data given in literature in [31] was unable to provide any information concerning this reported data point or how it was obtained. Density and conductivity results both show distinct non-linear trends

versus mixture mass percentage, as is common when mixing ionic liquids. When compared with a linear mixing law, there is a 100% over prediction of conductivity at 75% [Emim][$EtSO_4$]. This difference shrinks to a 78% and 42% for mixtures with 50% [Emim][$EtSO_4$] and 25% [Emim][$EtSO_4$] respectively. The other properties also exhibit non-linear mixing; however, the close property values of neat IL reduce the percent error.

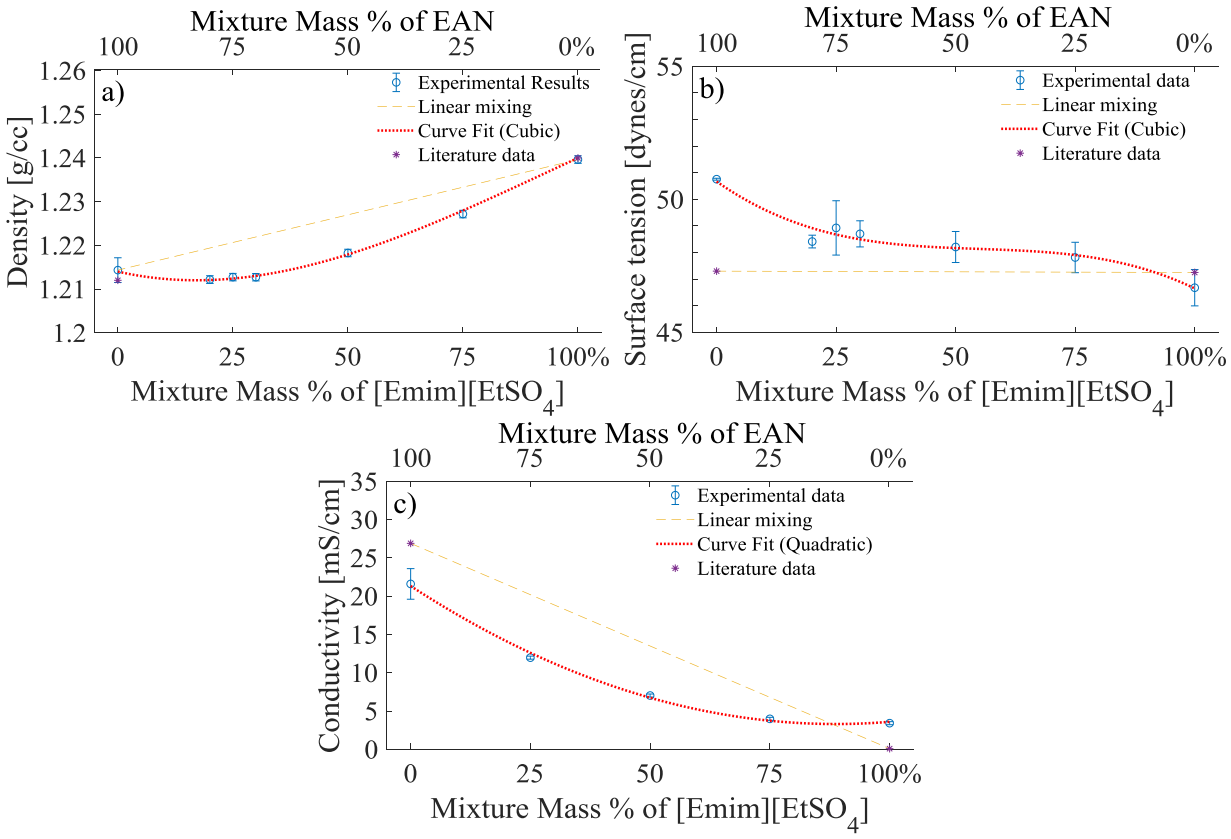

Fig. 4: Physical property measurements at various percentages of [Emim][$EtSO_4$] and EAN of a) density, b) surface tension, and c) conductivity

C. Mass spectra results

In this section, mass spectra of representative mixture mass percentages, flow rates, and angles during electrospray emission of the tested liquids are presented. The peaks shown in these spectra and specific cation and anion species associated with these peaks are identified. Information obtained from the spectrum analysis is also useful in clarifying how the observed m/q values change with mixture mass percentage of the mixtures.

Fig. 5 shows the spectra for three cases: neat [Emim][$EtSO_4$], neat [EAN], and a 50% by mass mixture of the two ionic liquids. Figure 5 a) and Fig. 5 b) provide results for anion and cation emission, respectively. These results are obtained at an off-axis-angle of 15° and a flow rate of 50 pL/sec for both neat [Emim][$EtSO_4$] and the 50% mixture, and at a flow rate of 3 nL/sec for neat EAN. The increased flow rate for EAN provides a reference to identify those peaks associated with EAN; EAN mass spectra information is unobtainable for both cation and anion modes at the low flow rate of 50 pL/sec due to EAN's volatility, as previously discussed [10, 33]. In Fig. 5, the x-axis is the mass-to-charge ratio (m/q). This corresponds to the amu of the species, assuming that the ions are singly charged. The y-axis represents the normalized relative counts. The normalization mixtures with [Emim][$EtSO_4$] is based on what are expected to be the n=0 [Emim][$EtSO_4$] emission species at 126 m/q for the anion mode and 111 m/q for the cation mode. Here, n refers to the number of neutral combinations attached to the ion, this is referred to as "degree of solvation," "aggregation number," or "number of neutrals" in literature. For these data sets (100% [Emim][$EtSO_4$] and 50% [Emim][$EtSO_4$] of Fig. 5), the counts have been normalized by the peak at 125-126 m/q for the anion mode and the peak at 111-112 m/q for the cation mode. The normalization for EAN is based on the 125 m/q anion peak because it aligned well with the normalization peak of the 100% [Emim][$EtSO_4$] while the 140 m/q

cation peaks was selected as it was the largest peaks above 100 m/q, which allowed it to be easily compared with the other spectra that were normalized by peaks over 100 m/q.

Figure 5 shows the neat spectra for [Emim][$EtSO_4$]. Peaks are clearly visible at 80, 98, 126, 143, and 361 m/q for the anion mode, and peaks at 81, 111, 138, and 348 m/q for the cation mode. In the neat [Emim][$EtSO_4$] anion spectra, the 361 m/q is the most intense followed by the 126, 98, 80, and 143 m/q peaks; the cation peaks, in order of descending intensity are 111, 348, 81, and 138 m/q.

Figure 5 also shows the neat spectra of EAN. Cation peaks are observed at 55, 84, 96, 112, and 140 m/q. The 55 m/q peak is difficult to pick out due to the proximity of it with the minimum reported m/q value. The 140 m/q peak is the largest, followed by the 84, 55, 112 and 96 m/q peaks respectively. Anion peaks are observed at 62, 78, 125, 151, 169, 187, 231, 279, 296, 340, and 384 m/q. In the anion data, the largest peak is at 62 m/q, followed by the 125, 164, 384, and 151 m/q peaks. The 62 m/q peak has about twice the number of counts as the 125 m/q peak.

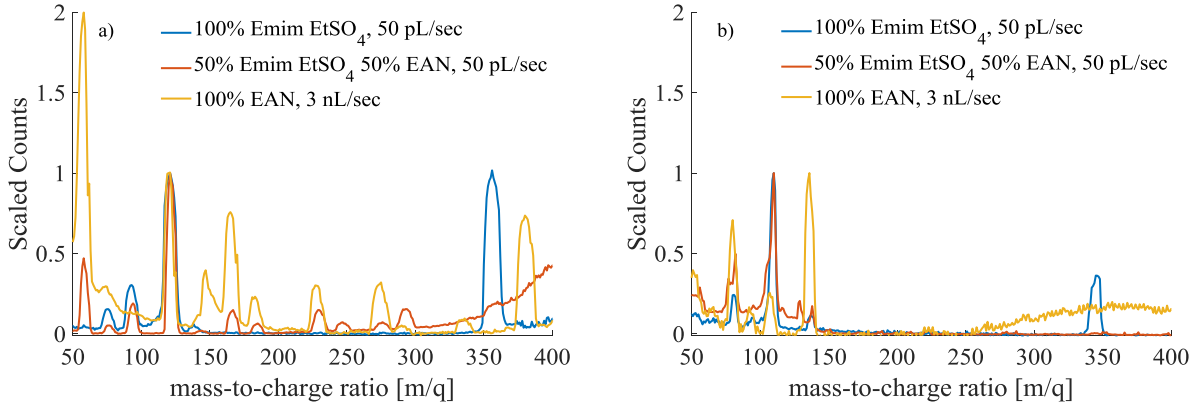

Fig. 5: Mass spectra of various % [Emim][$EtSO_4$] various % EAN and flow rates, 15° off axis for a) anion and b) cation emission modes

Fig. 5 also shows the spectra for the 50% [Emim][$EtSO_4$]/EAN mixture. The spectra show cation peaks at 55, 83, 111, 130, 139, 152, 173, 190, 211, 225, 281, and 345 m/q, while the anion spectra show peaks at 62, 79, 99, 126, 148, 171, 189, 233, 251, 280, and 297 m/q. At this mixture ratio, the largest peak is at 111 m/q for cation mode and 126 m/q for anion mode; note that these are also the normalization peaks. This result is similar to 100% [Emim][$EtSO_4$] where the 111 m/q peak is largest in cation mode and the 126 m/q peak is largest in anion mode, recall for 100% [Emim][$EtSO_4$] the 126 m/q was 98% of the largest peak present (at 361 m/q). It is interesting to further compare and contrast 50% [Emim][$EtSO_4$] spectra with 100% [Emim][$EtSO_4$] spectra. Unlike the 100% [Emim][$EtSO_4$] spectra, this 50% mixture does not show a peak at 361 or 348 m/q, which are among the largest of the 100% [Emim][$EtSO_4$] peaks. Additionally, the 50% [Emim][$EtSO_4$] mixture exhibits anion peaks at 189, 233, 251, 280 m/q and cation peaks at 130, 152, 173, 190, 211, 225, and 281 m/q, which are not present in the 100% [Emim][$EtSO_4$] spectra. The spectra presented in Fig. 5 clearly indicate that there are more species present in the 50% mixture than observed for 100% [Emim][$EtSO_4$]. It is also interesting to compare and contrast 50% [Emim][$EtSO_4$] spectra with neat (100%) EAN spectra. The anion 126 m/q peak in the 50% mixture is more than double that of the peak at 63 m/q, but in the neat EAN spectra the 63 m/q peak is double the 125 m/q peak . In cation mode for the 50% mixture, the 111 m/q peak is the largest with the peak at 83 m/q as second largest, and at about half the intensity. In contrast, for neat EAN, the 140 m/q peak is the largest and the 84 m/q peak is second largest at approximately 70% the intensity. Compared with the neat (100%) EAN spectra, the 50% mixture has additional anion peaks at 79, 99 148, and 251 m/q and additional cation peaks at 130, 152, 173, 190, 211, and 225 m/q. In addition, there are peaks from neat (100%) EAN not observed in the 50% mixture, namely the anion peak at 340 m/q and the cation peak at 96 m/q.

Fig. 6 presents the emission spectra at different angular orientation for the 50% [Emim][$EtSO_4$] mixture at 3 nL/s flow rate. The y-axis is again normalized as previously described. Fig. 6 a) and Fig. 5Fig. 6 b) show results for anion and cation emission modes, respectively. The general trends evident from Fig. 6 are that (1) there is a greater zero mass signal at low angles (e.g., 0°) due to droplets on centerline, this zero mass signal is evident as a baseline noise or inflation of the counts value at low m/q values, and (2) there is a reduction in intensity of all peaks with increase in off axis angle for both cation and anion mode. These qualitative trends in the angular dependence of the spectra agree with what has been described previously in literature [17]. Miller et al. [17], Chiu et al. [38], and Prince et al. [9] all show that as angle increases to larger off axis angles the peak intensity decreases. Miller et al.

[17] and Chiu et al. [38] both show that on centerline there is a larger amount of baseline noise or inflation of the counts value at low m/q. The mixture reported here appears to conform to expected qualitative electrospray trends with angular position.

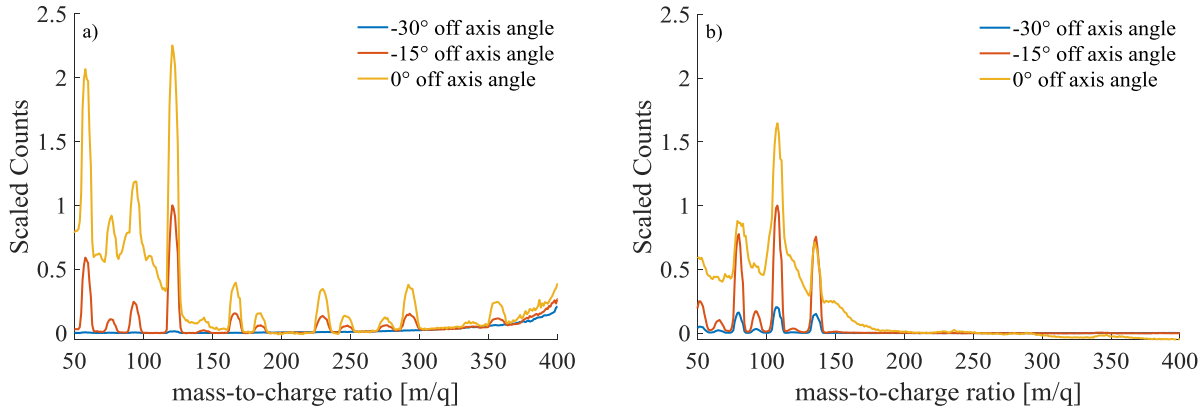

Fig. 6: 3 nL/s of 50% [Emim][EtSO$_4$] and 50% EAN by mass a) anion species emission at selected angles b) cation species emission at selected angles

D. Peak variations with mixture mass percentage

This section provides results that describe how the peaks in the mass spectra, and hence species present in the mixture, vary with mixture percentage. In Fig. 7, the x-axis is the mixture mass percentage of [Emim][EtSO$_4$] and the y-axis is the number of counts for specific peaks.. These peaks are of interest because the n=0 EAN species have anion and cation masses of 55and 62 m/q, respectively (shown in Fig. 7A), and n=0 anion and n=1 cation [Emim][EtSO$_4$] species have masses of 126 (n=0 [EtSO$_4$] monomer) and 348 m/q (n=1 dimer [Emim]+[Emim][EtSO$_4$]), respectively (shown in Fig. 7B). Also, these peaks are chosen because they are among the dominant peaks in the spectra, as seen in Fig. 5 and Fig. 6, and are formed only from ions of the IL being investigated. The [Emim]$^+$[Emim][EtSO$_4$] cation dimer was chosen over the [Emim]$^+$ monomer because the [Emim]$^+$ peak is at 111 m/q and may be convoluted by the n=1 proton transferred EA species since its mass is 112 m/q. The intensities of these peaks are plotted for the 50 pL/sec and -30° off axis case vs. mixture mass percentage. This flow rate was selected as a large population of ions is observed at this flow rate. The -30° off-axis-angle was chosen to limit the amount of noise, from centerline, in the signal as much as possible. Since, as previously discussed, neat EAN does not electrospray at the low flow rates investigated here, the figure does not include data for neat (100%) EAN.

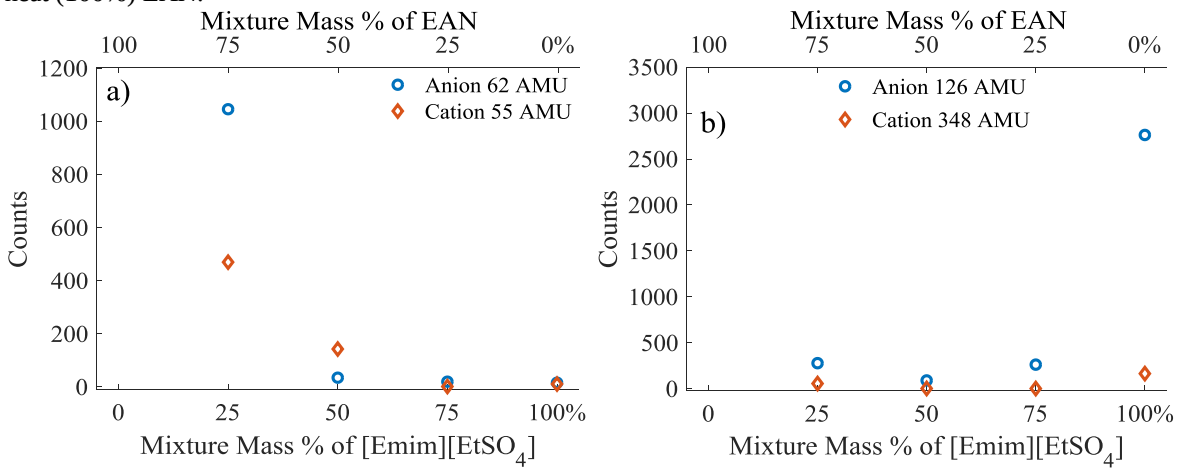

Fig. 7: Counts vs. mixture mass percentage of selected peaks at 50 pL/sec, -30° off axis for specific a) EAN and b) Emim peaks

As Fig. 7 shows, the counts of a particular species increases with increasing concentration of that species in the mixture. In particular, Fig. 7A shows that as the mixture mass percentage of [Emim][EtSO$_4$] increases and the

mixture mass percentage of EAN decreases, the number of counts for the EAN n=0 peaks decrease to essentially baseline noise levels at the 100% [Emim][$EtSO_4$] level. It appears from Fig. 7A that changing the mixture ratio from 25 to 50% has a significant effect on the counts of the 62 m/q anion and 55 m/q cation species of EAN. As the mixture ratio increases from 25 to 50%, the 62 m/q anion counts decrease from 1046 counts to 35, and the 55 m/q cation counts decreases from 470 to 143, respectively. This is the largest decrease across all mixture ratios investigated. Fig. 7B shows that as mixture mass percentage of [Emim][$EtSO_4$] increases, the counts of species associated with [Emim][$EtSO_4$] also increases, with the 126 m/q peak increasing more than the 348 m/q peak. Fig. 7B also shows that the greatest increase in counts of these species occurs when the mixture ratio increases from 75 to 100%. Specifically the 126 m/q anion increases from a counts value of 263 to 2762 as the mixture ratio increases from 75% to 100%, while the 348 m/q cation only increases from 3 to 165, respectively.

Table 1 and Table 2 provide tabulated lists of the peaks observed in the spectra for the different mixture ratios investigated, for anion and cation modes, respectively. The criteria for reporting a peak as present is a signal to noise ratio greater than 2. The noise level value is taken as the baseline signal value to the right of the peak. This criteria was used rather than selecting a specific m/q value to the right as different peaks have different finite widths and in some areas multiple peaks are present relatively close together, for instance if 8 m/q was selected the peak at 169 m/q would be the "error" for the 161 m/q peak creating for 25% [Emim]][$EtSO_4$] and the peak at 161 would be incorrectly omitted. The peaks shown are from spectra acquired at 15° off axis in order to avoid a large baseline due to droplets on/near centerline; also these results correspond to a nominal flow rate of 50 pL/sec. Peaks for EAN are taken from the 3 nL/sec case because stable low flow rates were not achievable for both modes at 50 pL/sec due to the volatility of EAN. In addition, in both tables identify anticipated species that align with the peaks observed in the spectra. A specific species is assigned to a peak by considering all known ions and neutrals present in the liquid and then determining the possible m/q values of all combinations of these ions and neutrals. When multiple ion/neutral combinations (species) are possible for a given peak, within a tolerance of 3 m/q, all the possible unique species fitting this criteria are then reported in the table. References to other literature sources that have identified the presence of indicated species are also provided in the rightmost columns of these two tables.

1) Anion spectra results (Table 1)

Table 1 shows that observed peaks for neat (100%) [Emim][$EtSO_4$] anion emission are at 80, 98, 126, 143, and 361 m/q. Many of these peaks clearly correspond to expected species based on the composition of [Emim][$EtSO_4$], when noting its ionic form (see Fig. 1), as well as species associated with chemical reaction. These reaction-generated species will be discussed subsequently. The [$EtSO_4$] anion is present at 126 m/q and at 361 m/q is shown to be bonded with the [Emim][$EtSO_4$] neutral pair. The [HSO_4] anion appears at 98 m/q and at 143 m/q bonded with a neutral ethanol. Evidence of both of these species in [Emim][$EtSO_4$] have been observed in literature [39]. Finally, the 80 m/q peak has been seen previously in [Emim][$EtSO_4$] spectra [6] (work directly related to the present investigation) and is labeled as "species from [Emim][$EtSO_4$]" as this m/q value does not align with any known combination of possible species. This 80 m/q peak may be due to a molecular fragment or impurities in the liquid.

In Table 1, the observed peaks for neat (100%) EAN anion emission are 62, 78, 125, 151, 169, 187, 231, 279, 296, 340, and 384 m/q. Many of these peaks clearly correspond to expected species based on the composition of EAN, both in its ionic and proton transferred forms (see Fig. 1). The nitrate anion [NO_3] is present at 62 m/q, while nitrate bonded with nitric acid [HNO_3] is evident at 125 m/q. This species has been seen previously in 2-Hydroxyethylhydrazinium Nitrate (HEHN) [9]. Peaks at 169 and 187 m/q appear to be nitrate bonded with two ethylamine [EA-H] molecules and nitrate bonded with two nitric acid molecules [HNO_3], respectively. The peak at 231 m/q indicates that nitrate is bonded with an entire EAN molecule and ethylamine [EA-H]. At 296 m/q, this peak is identified as nitrate bonded with 2 EAN molecules. The peaks at 78, 151, 279, 340, and 384 m/q are then labeled as "species from EAN" because no combination of known potential species gives rise to those m/q values. As discussed earlier, the species corresponding to these peaks may be fragments, fragments bonded with other species, and/or impurities in the liquid.

Three different mixtures of [Emim][$EtSO_4$] with EAN are reported in Table 1 corresponding to mixture ratios of 75%, 50%, and 25% [Emim][$EtSO_4$]. Some of the identified peaks and species are present in all three mixtures, while others are only identified for specific mixture ratios. The species common to all mixture ratios will be discussed first, followed by discussion of those species that are unique to each mixture ratios. Nitrate [NO_3], an unknown species from [Emim][$EtSO_4$] at 80 m/q, hydrogen sulfide [HSO_4], [$EtSO_4$], and hydrogen sulfide bonded with methanol ([HSO_4]+4[C_2H_5OH]) are each present for all intermediate mixture ratios. A proton transferred form of nitrate (nitric acid, [HNO_3]) may also be present at 125 m/q for all intermediate mixture ratios but cannot be conclusively identified due to its proximity to the peak at 126 m/q [$EtSO_4$].

Table 1: Mass-to-charge ratio of anion peaks and corresponding species identified in the mass spectra of mixtures of 100, 75, 50, 25, & 0% by mass [Emim][$EtSO_4$] with EAN

100	75	50	25	0	% [Emim][$EtSO_4$]	Reference values	
[m/q]	[m/q]	[m/q]	[m/q]	[m/q]	Species	Ref.	Ref. Liquid
	62	63	62	62	[NO_3]	--	--
				78	Species from EAN	--	--
80	79	79	80		Species from [Emim][$EtSO_4$]	[40]	--
98	100	99	98		[HSO_4]	[39, 40]	[Emim][$EtSO_4$] [$EtSO_4$] in urine
	125*	125*	125*	125	[NO_3]+[HNO_3]	[6]	HEHN
126	126	126	126		[$EtSO_4$]	[40]	[$EtSO_4$] in urine
143					[HSO_4]+[C_2H_4OH]	[6]	[Emim][$EtSO_4$]
	147	148			Species from [Emim][$EtSO_4$]	[6]	[Emim][$EtSO_4$]
			151	151	Species from EAN	--	--
			161		[HSO_4]+[HNO_3]	--	--
		171	169	169	[NO_3]+2[EA-H]	--	--
				187	[NO_3]+2[HNO_3]	[6, 37]	HEHN
		189	189		[NO_3]+2[HNO_3] or [$EtSO_4$]+[HNO_3] or [HSO_4]+2[C_2H_5OH]	[37]	EAN
				231	[NO_3]+[EA-H]+[EA+NO_3]	[37]	EAN
		233			[NO_3]+[EA-H]+[EA+NO_3] or [HSO4]+3[C_2H_5OH]	[37]	EAN
			237		[NO_3]+[Emim+NO_3]		
		251	255		[$EtSO_4$]+2[HNO_3]	--	--
				279	Species from EAN	[37]	EAN
	280	280	281		[HSO_4]+4[C_2H_5OH]	[6]	[Emim][$EtSO_4$]
				296	[NO_3]+2[EA+NO_3]	--	--
		297	298		[NO_3]+2[EA+NO_3] or [$EtSO_4$]+[EAN]+[EA-H]	--	--
			323		[NO_3]+[EA+NO_3]+[HSO_4+Emim] or [$EtSO_4$]+[EA-H]+[HSO_4+EA]	--	--
				340	Species from EAN	--	--
	360				[$EtSO_4$]+[EA+NO_3]+[EA+NO_3] or [$EtSO_4$]+[Emim+$EtSO_4$] or [NO_3]+[HNO_3]+[Emim+$EtSO_4$]	--	--
361					[EtSO4]+[Emim+$EtSO_4$]	[6]	[Emim][$EtSO_4$]
			362		[NO_3]+[HNO_3]+[Emim+$EtSO_4$]	--	--
				384	Species from EAN	[37]	EAN

*Denotes a peak potentially embedded in a more pronounced peak.

At a mixture ratio of 75% [Emim][$EtSO_4$], in addition to the species discussed above that are common to all mixture ratios, two other peaks are identified at 147 and 360 m/q. The 147 m/q peak does not match any expected combination of species. The 360 m/q peak could be associated with the reactions [$EtSO_4$]+2EAN, [$EtSO_4$]+[Emim][$EtSO_4$], or [NO_3]+[HNO_3]+[Emim][$EtSO_4$].

At a mixture ratio of 50% [Emim][$EtSO_4$] six additional peaks, not generally found in all other mixture ratios, are identified at 148, 171, 189, 233, 251, and 297 m/q. The peak at 148 is also provisionally present for the 75% mixture at 147 m/q. It does not match any expected or known combination of species. The peak at 171 m/q may be [NO_3]+2[EA-H] and is also observed in the 25% [Emim][$EtSO_4$] mixture and neat (100%) EAN. The peak at 189 m/q also appears in the 25% mixture and may correspond with nitrate bonded with two proton transferred nitrates ([NO_3]+2[HNO_3]), or with [$EtSO_4$] bonded with a proton transferred nitrate ([$EtSO_4$]+[HNO_3]), or with hydrogen sulfide bonded with two ethanol neutrals ([HSO_4]+2[C_2H_5OH]). The peak at 233 m/q corresponds to either

$[NO_3]$+[EA-H]+$[EA+NO_3]$ or [HSO4]+3$[C_2H_5OH]$; this is similar to the 231 m/q peak in neat EAN that is attributed to $[NO_3]$+[EA-H]+$[EA+NO_3]$. The peaks at 251, 280, and 297 m/q appear in both 50% and 25% mixture ratios and correspond to species associated with $[EtSO_4]$+2$[HNO_3]$, $[HSO_4]$+4$[C_2H_5OH]$, and either $[NO_3]$+2$[EA+NO_3]$ or $[EtSO_4]$+[EAN]+[EA-H].

At a mixture ratio of 25% [Emim][$EtSO_4$] there are ten peaks in addition to those peaks common to all three mixture ratios. This particular mixture ratio has the highest number of identifiable peaks. The ten additional peaks occur at 151, 161, 169, 189, 237, 255, 281, 298, 323, and 362 m/q. The peak at 151 m/q also appears in pure EAN and is described as "species from EAN" as no expected combination of ion and neutrals aligns with this mass. The peak at 161 m/q corresponds to hydrogen sulfide and proton transferred nitrate ($[HSO_4]$+$[HNO_3]$). The peak at 169 m/q aligns with $[NO_3]$+2[EA-H] and is also observed in the 50% [Emim][$EtSO_4$] mixture and neat EAN. The peak at 189 m/q also appears in the 50% mixture and may correspond with $[NO_3]$+2$[HNO_3]$ or $[EtSO_4]$+$[HNO_3]$ or $[HSO_4]$+2$[C_2H_5OH]$. The peak at 237 m/q is similar to that present at 233 m/q in the 50% mixture; however, it is shifted 4 m/q higher. This suggests a composition of $[NO_3]$+[Emim+NO_3]. The peaks at 255, 281, and 298 m/q also appear in the 50% mixture ratio and correspond to species $[EtSO_4]$+2$[HNO_3]$, $[HSO_4]$+4$[C_2H_5OH]$, and either $[NO_3]$+2$[EA+NO_3]$ or $[EtSO_4]$+[EAN]+[EA-H]. The peak at 323 m/q corresponds to either $[NO_3]$+$[EA+NO_3]$+[HSO_4+Emim] or $[EtSO_4]$+[EA-H]+[HSO_4+EA]. Finally, the peak at 362 m/q appears to correspond with $[NO_3]$+$[HNO_3]$+[Emim+$EtSO_4$]. For this peak, the alternative species n=1 $[EtSO_4]$+[Emim+$EtSO_4$] is not likely since there is not a corresponding peak in the 50% mixture

2) Cation spectra results (Table 2)

Table 2 provides results for observed cation spectra peaks; organization of the table follows that as describes for Table 1. Table 2 indicates that peaks are observed for 100% [Emim][$EtSO_4$] at 81, 111, 138, and 348 m/q. These peaks align with either anticipated or previously reported data. The 111 m/q peak is [Emim]. The 348 m/q peak is [Emim]+[Emim+$EtSO_4$]. The peaks at 81 and 138 m/q do not align with anticipated species, so these peaks are reported in the table as "species from [Emim][$EtSO_4$]," However, all four of these peaks have been previously observed and identified with species emitted from [Emim][$EtSO_4$] by Wainwright et. al [6].

Table 2: Mass-to-charge ratio of cation peaks and corresponding species identified in the mass spectra of mixtures of 100, 75, 50, 25, & 0% by mass [Emim][$EtSO_4$] with EAN

100	**75**	**50**	**25**	**0**	**% [Emim][$EtSO_4$]**	**Reference values**	
[m/q]	**[m/q]**	**[m/q]**	**[m/q]**	**[m/q]**	**Species**	**Ref.**	**Ref. Liquid**
	54			55	[EA]	[22]	Dopamine
	68				Species from [Emim][$EtSO_4$]	[6]	[Emim][$EtSO_4$]
81	82	83	83		Species from [Emim][$EtSO_4$]	[6]	[Emim][$EtSO_4$]
				84	Species from EAN	--	--
				96	Species from EAN	--	--
111	111	111	111		[Emim]	[6, 38]	[Emim][Im]
	112*	112*	112*	112	[EA]+[EA-H]	--	--
		130			--	--	--
138	139	139			Species from [Emim][$EtSO_4$]	[6]	[Emim][$EtSO_4$]
			140	140	Species from EAN	--	--
		152	155		[EA]+[EA-H]+$[C_2H_5OH]$	--	--
		173	175		[Emim]+$[HNO_3]$	--	--
		190			--	--	--
		211			[Emim]+[EA-H]+$[C_2H_5OH]$	--	--
			216		[Emim]+[EA-H]+[EA-H]	--	--
		225			[EA]+[EA-H]+$[EA+NO_3]$	--	--
		281	283		[Emim]+[EA-H]+ $[EA+NO_3]$	--	--
348	348	345	347		[Emim]+[Emim+$EtSO_4$]	[6]	[Emim][$EtSO_4$]

*Denotes a peak potentially embedded in a more pronounced peak.

Cation peaks are observed for neat (100%) EAN at 55, 84, 96, 112, and 140 m/q. The [EA] cation (ethylammonium) is present at 55 m/q and has been identified previously in an investigation of dopamine [22]. Proton transferred ethylamine ([EA-H]) is evident at 112 m/q, with the ethylammonium cation. The peaks at 84, 96, and 140 m/q are not anticipated based on composition of known ions and neutrals. These peaks are labeled as "species from EAN".

The intermediate mixture mass percentages are for 75%, 50%, and 25% [Emim][$EtSO_4$]. There are common species present at 82, 111, 112, 139, 140, and 347 m/q. The peaks at 82, 139, and 140 m/q have all been assigned as either "species from EAN" or "species from [Emim][$EtSO_4$]." The peaks at 111 and 112 m/q are attributed as [Emim] and [EA]+[EA-H] respectively. Some overlap between these species is expected however [Emim] is expected to be the dominant species since it also appears as the dominant species in both the 100% [Emim][$EtSO_4$] and 50% [Emim][$EtSO_4$] case but not in the neat EAN case. The 347 m/q peak coincides well with the anticipated species [Emim]+[Emim+$EtSO_4$]. Peaks for 75% [Emim][$EtSO_4$] mixture are reported at 54, 68, 82, 111, 139, and 348 m/q, with no species indicated that are not common with the 50% and 25% mixtures.

The 50% [Emim][$EtSO_4$] mixture has peaks at 130, 152, 173, 190, 211, 225, 281 m/q not identified as common with both other mixtures. The 130 m/q peak is unique only to this mixture and does not appear to correspond with anticipated species or species in pure liquids. The peaks at 152 and 173 m/q for this 50% mixture ratio case are also provisionally identified with peaks at 155 and 175 m/q in the 25% mixture. These are assigned as [EA]+[EA-H]+[C_2H_5OH] and [Emim]+[HNO_3] respectively. The 211, 225 and 281 peaks are assigned as [Emim]+[EA-H]+[C_2H_5OH], [EA]+[EA-H]+[EA+NO_3], and [Emim]+[EA-H]+[EA+NO_3] respectively. The 25% [Emim][$EtSO_4$] case peaks that are not common to all three mixtures are observed at 155, 175, 216, 283 m/q. The peaks at 216 m/q is the only peak not previously identified for the 50% mixture; it is attributed to the [Emim]+[EA-H]+[EA-H] species.

V. Analysis & Discussion

In this section, different aspects of mixture ratio effects as related to propellant design are analyzed and discussed. First, the impacts that the physical chemistry results have on the predicted performance of these ionic liquids as electrospray propellants are presented and applications to optimizing propellant composition is discussed. Second, the effects that species observed in the mass spectra have on propulsion performance are discussed. Finally, discussions are provided regarding how the liquid changes with varying mixture mass fraction in terms of 1) chemical makeup, due to internal neat IL chemical reactions, 2) microscopic structure, due to the shift in inter-molecular interactions as the composition changes, and 3) species plume composition.

A. Performance predictions based on physical chemistry results

In this section, performance predictions based on the measured physical properties, presented above, are shown and compared with those based on linear mixing rules. Performance predictions based on linear mixing rules over predict performance when compared to those based on linear mixing rules. The physical properties measured and presented in Section V of this work show several non-linear trends. The properties (density, surface tension, and conductivity.) were selected for study as they are all inputs to the electrospray performance equations (see equation 1 and 2) as presented by J.F. de la Mora [41]. Equation 1 relates the current emitted by the cone jet ($I(Q)$) to the surface tension (γ), conductivity (K), liquid flow rate (Q), dielectric constant (ε), and a function of the dielectric constant $f(\varepsilon)$; however, it does not include any mass loss from volatility. The surface tension and conductivity measurements have been described (in Fig. 4). The dielectric constant is based on a linear interpolation of the results presented by Huang due to the fact that dielectric constants are difficult to obtain for conductive liquids [42]. Linear mixing based on mixture mass percentage is further supported by Heid, et. al. [43], who investigated variation of dielectric constant for two different ([Emim][DCA] and [Emim][OTF]) at various mixtures with water. When the molarity based results from Heid [43] are converted to mixture mass percentage of IL, the linear curve fits for both of these liquids with water have R^2 values greater than 0.98, suggesting that this property is captured well by assuming linear mixing for [Emim]-based ILs. The functional dependence on the dielectric constant ($f(\varepsilon)$) is taken directly from [41], which has sufficient information for the range of ($f(\varepsilon)$) relevant to this study. This physical property information set is then utilized to predict the electrospray propulsion performance as follows. From the measured values of the properties and an assumed flow rate of 50 pL/sec, the anticipated emission current can be calculated directly via equation 1,

$$I(Q) = f(\varepsilon)\left[\frac{\gamma K Q}{\varepsilon}\right]^{.5} \quad (1).$$

From this expected current, the thrust (F) can be computed with equation 2. When using this calculation, a representative accelerating voltage of 2.3 kV is used. The mass flow rate is based on the prescribed volumetric flow rate and experimentally determined density provided in Fig. 4.

.

$$F = \sqrt{2 V_{acc}\, \dot{m}\, I} \qquad (2).$$

Fig. 8 shows the results of these calculations based on thwo different input data sets: 1) the experimentally measured physical property values across the mixture mass fraction range given in Fig. 4.

and 2) assuming linear mixing based on the experimentally measured values for the neat liquids. In Fig. 8, the x-axis corresponds to the varying mixture mass percentages of liquids in the mixture. The mass percentage range provided on the top of the plot is associated with EAN. The bottom mass percentage range is associated with [Emim][$EtSO_4$]. In Fig. 8 the y-axis in a) reports current (in μ amps) based on equation 1, while the y-axis in b) corresponds to the predicted thrust based on equation 2. As noted earlier, for both approaches, a linear variation in the dielectric constant was assumed for all of this analysis. Since the bulk of the mixture conductivity values utilized in the linear mixing approaches at intermediate mixture mass fractions are associated with EAN (note that the conductivity of neat EAN is over 6 times that of neat [Emim][$EtSO_4$]), the two sets of linear mixing results thus provide similar results, due to the similarity in EAN conductivity, except for neat [Emim][$EtSO_4$] where the conductivity of EAN does not contribute to the mixture conductivity, by definition.

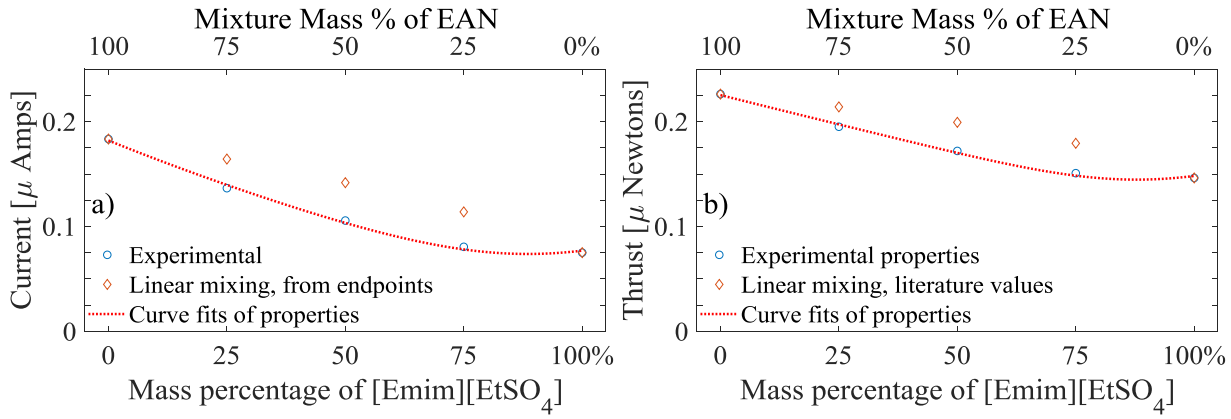

Fig. 8: Current emission (a) and thrust performance (b) of different mixture mass percentages based on experimental data of Fig. 4, , assuming linear mixing of literature reported physical properties, and assuming linear mixing of experimentally obtained physical properties for the neat ionic liquids.

Figure 8 shows that, at intermediate mixture mass fractions, the performance (both in terms of thrust and emission current) based on actual experimental data obtained in the present study are significantly below the performance based on a linear mixing assumption. The difference is due to the non-linear mixing, and is mainly due to the conductivity. For the two ionic liquids investigated here there is a large difference in conductivity such that the conductivity changes non-linearly over approximately an order of magnitude. Assuming linear mixing results in a 40% overestimation in predicted performance at 75% [Emim][$EtSO_4$]. The percent differences for the 50% and 25% [Emim][$EtSO_4$] compositions are approximately 35 and 20%, respectively. This discrepancy demonstrates the importance of obtaining intermediate experimental property values when predicting propulsive performance for mixtures. This analysis and discussion does not consider the effect of liquid mass loss from evaporation due to liquid volatility.

Mixture property data vary non-linearly with mixture mass percentage and this means predicted electrospray performance will have an extrema at some mixture mass percentage. For the mixtures presented here, due to the negative concavity of the conductivity versus mixture mass percentage (see Fig. 4), the performance predictions will yield a distinct minima. However, it is important to note that mixtures of other liquids could, in fact, provide a positive concavity in the conductivity data, thus yielding a maximum in performance at a specific mixture mass percentage. In their numerical and experimental investigation on various mixture percentages of one protic (EAN) and one aprotic ionic liquid ([Emim][BF_4]), Docampo-Álvarez et al [3] found experimental density to be concave with mixture ratio and a local maxima in conductivity. This would yield a local performance maximum.

Local minima (or maxima) in predicted current, thrust, and specific impulse, based on currently presented results, are found using polynomial curve fitting of the physical properties. Specifically, in the present analysis, a cubic function is used and fit to the density and surface tension data, as shown in Fig. 4. A quadratic function is fit to conductivity data, as shown in Fig. 4. The forms of these curve fits were chosen based on the goodness of fit parameter for various polynomial curve fits, i.e. how well the polynomial curve fit represented the data. These curve fits provide good representations (with the goodness of fit parameter, R^2, values > 0.95) of the physical property data. They yield predicted minima points for the performance metrics by utilizing equations 1 and 2. Specific impulse of the thruster can then be found from ($I_{sp} = \frac{T}{\dot{m}\, g_0}$) For the present work, the mixture mass percentages for minimum current, thrust, and specific impulse are found using these curve fits to be 88.5%, 87.2% and 89.1% [Emim][$EtSO_4$], respectively. The values of current, thrust, and specific impulse at these mixture ratios are 0.074 μA, 0.15 μN, and 240 seconds, respectively. These values are not significantly different from the 75% and 100% [Emim][$EtSO_4$] mixture ratios reported in Fig. 8 For example, the minimum thrust is only 1.1% lower than the predicted value at a 100% [Emim][$EtSO_4$] mixture ratio. This difference is near the uncertainty of the physical property measurements, which is 1-2% based on repeatability (standard deviation). Liquids with more disparate density would have larger differences in the mixture ratios corresponding to optimum current, thrust, and specific impulse. Further, the values of those performance metrics at the extrema will be impacted by the relative difference in property values between the liquids. In general, these results indicate that when optimizing performance using liquids with nonlinear mixture characteristics, the predicted optimal mixture for current, thrust, and specific impulse will occur at different intermediate mixture ratios if the densities are different and obtaining intermediate predictions based on intermediate property measurements may be important.

B. Comparison of [Emim][$EtSO_4$] electrospray mass spectra with literature

This section compares the spectra results and assigned species with what has been seen previously in literature. First, comparisons between the neat [Emim][$EtSO_4$] results resented here to those seen previously in this setup are made. Then chemical reactions within the ionic liquids are described, and evidence of the product species of these reactions is presented.

The neat [Emim][$EtSO_4$] anion mode spectra, Fig. 5a, has characteristics similar but not identical to results shown in earlier work [6]. The notable difference is that the previous identified spectra peaks that are not present in the results here. Anion mode peaks are missing at 65 and 280 m/q in the present work, and there is a much more pronounced peak at 361 m/q identified here. For the cation spectra for [Emim][$EtSO_4$], peaks are missing at 55, 69, and 95 m/q. It is unclear why these peaks were present in the previous spectra [6] and not present now. Previous work attributed these peaks to ion fragments and/or impurities, because their mass does not correlate with any expected ion species based on the parent anion/cation constituents. One possible explanation for the presence or lack thereof of these peaks is that the data of Fig. 5 were obtained with a newer batch of [Emim][$EtSO_4$]. The data presented here were acquired within three months after receiving the [Emim][$EtSO_4$], while spectra from previous work [6] were acquired over a year after receiving. [Emim][$EtSO_4$] is known to slowly decompose over time, especially in the presence of water (decomposed products are identified in these spectra), which may bolster the hypothesis that these peaks are due to decomposition products (i.e., impurities), the concentration of which may increase over time.

Chemical reactions within the liquids investigated here give rise to additional species that are observed in the electrospray plume. This work has identified at least one chemical reaction for each liquid, the products of which appear to be in the spectra. Specifically, proton-transfer is known to occur in EAN and this chemical reaction is written as equation 3, while [$EtSO_4$] is known to decompose in the presence of water according to the reaction give in equation 4. The proton reaction in EAN involves a hydrogen atom transferring from the ethylammonium cation to the nitrate anion thus forming ethylamine and nitric acid [26-28]. Similar cation to anion proton transfer has been seen in other similar ILs, namely HAN and HEHN [6, 9, 21]. The water-[$EtSO_4$] reaction involves water reacting with [$EtSO_4$] to form hydrogen sulfide [HSO_4] and ethanol, this has been seen previously in [39].

$$[EA] + [NO_3] \xrightarrow{yields} [EA - H] + [HNO_3] \tag{3}$$

$$H_2O + [EtSO_4] \xrightarrow{yields} [C_2H_5OH] + [HSO_4] \tag{4}$$

In Table 1 and Table 2 correlate the mass of these product species with observed peaks in the spectra. EAN is observed to emit proton transfer species, which are the products of reaction 1. These species are clearly present at 125 m/q in the anion mode and 112 m/q in the cation mode for the species $[NO_3][HNO_3]$ and $[EA][HNO_3]$. Additionally, proton transfer species from EAN are present at 161, 169, 187, 231, 251, 255, 297, and 362 m/q in the anion mode and 155, 175, 216, 225, 283 m/q in the cation mode. This proton transfer on the nitrate functional group is expected for a PIL and is similar to the results previously seen by Wainwright and Prince [6, 9]. In contrast to Wainwright's previous results with $[Emim][EtSO_4]$ and HAN, proton transferred species are also present in cation mode. This means that the proton transferred species are binding to both anions and cations during emission, suggesting these species are next to each other in the mixture. There is also evidence of the $[EtSO_4]$-water reaction, equation 2. This is most evident as a peak at 98 m/q in the anion spectra due to $[HSO_4]$ (theoretical mass of 97m/q). Additional evidence of this reaction is also present at 143 m/q, as both products of Ficke's reaction ($[HSO_4]+[C_2H_5OH]$) are observed in combination. More evidence of $[HSO_4]$ is also found at 161 and 281 m/q for anion mode, where $[HSO_4]$ is paired with $[HNO_3]$ and $4[C_2H_5OH]$ respectively, Table 1. Evidence of ethanol presence in the cation plume at 155 and 211 m/q as both of these cation emissions require neutral ethanol, in order to account for these m/q values. Potentially most interesting is the peak at 161 m/q, anion mode, that requires reaction products from both anticipated reaction to form ($[HSO_4]+[HNO_3]$).

Reaction product species are evidenced in the plume from both a reaction from water and $[EtSO_4]$ and a proton transfer reaction between the EAN ions, the proton transfer reaction of EAN is potentially aided by water [27, 28], which provides more species in the plume and more neutrals in the liquid. As the charge carrying ions are reduced to neutrals this will result in a reduced conductivity, as observed by the Nernst-Einstein equation, and hence reduced performance, seen in Equation 2 and Fig. 8. Additionally, the presence of the $[HSO_4]$ anion adds another lighter anion; this appears at roughly 20% of the strength of the $[EtSO_4]$ peak suggesting that models assuming only $[EtSO_4]$ emission for neat $[Emim][EtSO_4]$ will over predict the average mass of emitted species by 6 amu, representing a 5% change in m/q. This extra anion will also change the organization structure of the liquid. The presence of products from this reaction, as evidenced by these spectra peaks, indicate that limiting the exposure of $[Emim][EtSO_4]$ to water is of paramount importance, the same is true for EAN as water may aid in proton transfer [27]. Models for these liquids should include presence of both proton transfer and $[EtSO_4]$+water reaction products.

VI. Conclusions

Mixtures of two ionic liquids ($[Emim][EtSO_4]$ and EAN) are examined in terms of their mixture properties and the impact on predicted electrospray propulsive design and performance. It is found that it is important to use the actual physical properties of the mixtures, particularly in order to correctly determine optimal mixing ratios. The physical chemistry properties obtained in this study for the (individual) selected ILs agree well with literature data. The use of actual intermediate mixture values of properties, however, is shown to be necessary when predicting the propulsive performance of mixtures of ILs. Specifically, this study shows a large discrepancy (~40%) between predicted performance based on the common assumption of linear mixing and actual mixture properties. These discrepancies arise in the analytic performance prediction model and do not capture evaporation/volatility effects that are observed. Additionally, it is important to note that optimal mixture ratio for current emission, thrust, and specific impulse will be different if mixture density is not constant across mixture ratios.

Plume mass spectra of four different mixture mass percentages of $[Emim][EtSO_4]$ and EAN are directly compared at 50 pL/sec for both cation and anion emission modes. Neat EAN spectra at 3 nL/sec are also discussed for both of these emission modes in order to identify peaks specific to EAN. Anticipated species are assigned to these peaks. Comparison of the spectra suggests that the quantity of a species in the ionic liquid might relate to the composition of the plume. But this study only focused on four specific ion species, and did not include the droplets, nor did it compare the total [Emim] species versus the total EAN species. Additionally, each of the four mixture mass percentages of $[Emim][EtSO_4]$ and EAN for which flow rate effects are measured show similar qualitative trends to that seen in previous work for both flow rate and angle [17]. Species swapping where anions from one IL are emitted with cations from the other appear to be present in the spectra. Additionally, EAN is found to emit proton transferred species in both cation and anion modes when in mixture with $[Emim][EtSO_4]$, and emitted along with $[Emim][EtSO_4]$ in both modes. Proton transfer species may reduce conductivity due to fewer charge carrying ions, and thus change the average mass-to-charge ratio of species. Changes in the average mass-to-charge ratio would also change expected performance.

Results of this study show that, when isolated in a chamber, neat EAN has an approximate 50% increase in base pressure when compared to the mixture comprised of 75% EAN and 25% $[Emim][EtSO_4]$ (by mass). For this same

mixture percentage, EAN emission at low flow rates is obtained. This is in contrast to the difficulty of successfully electrospraying neat EAN (due to its tendency to evaporate). This study indicates that even with the relatively small amount of [Emim][$EtSO_4$] represented in a 75% EAN/25% [Emim][$EtSO_4$] mixture, EAN is still present in the plume at low flow rates, thus suggesting that in the mixture, EAN is not simply boiling off at this mixture mass percentage, leaving [Emim][$EtSO_4$] to be emitted on its own. This result suggests that PILs with finite volatility may be useful as electrospray propellants by pairing them with AILs or other liquids whose vapor pressures are negligible.

Acknowledgments

Support for this work was provided through the NASA Marshall Space Flight Center, NASA grant NNM15AA09A, and the Air Force University Nano-satellite Program through the Utah State University Research Foundation, grant CP0039814. Additional support was provided by NASA Goddard Space Flight Center through the NASA Undergraduate Student Instrument Project grant NNX16AI85A, and the University of Missouri System Fast Track Program, FastTrack-16003R. M. Wainwright thanks the Department of Education for their Graduate Assistance in Areas of National Need Fellowship P200A150309, AFRL Kirtland,and both Jaykob Mazer and Dr. David Riggins at Missouri S&T for their help in preparing the manuscript.

References

[1] Chatel, G., Pereira, J. F. B., Debbeti, V., Wang, H., and Rogers, R. D. "Mixing Ionic Liquids-"Simple Mixtures" or "Double Salts"?," *Green Chemistry* Vol. 16, No. 4, 2014, pp. 2051-2083. doi: 10.1039/c3gc41389f

[2] Greaves, T. L. a. D., C.J. "Protic Ionic Liquids: Properties and Applications," *Chemistry Reviews* Vol. 108, 2008. doi: 10.1021/cr068040u

[3] Docampo-Ãlvarez, B., Gómez-Gonzãlez, V., Mẽndez-Morales, T., Rodrígues, J.R., López-Lago, E., Cabeza, O., Gallego, L.J. and Varela, L.M. "Molecular dynamics simulations of mixtures of protic and aprotic ionic liquids," *Physical Chemistry Chemical Physics* Vol. 18, 2016, pp. 23932-23943. doi: 10.1039/c6cp03700c

[4] Fumino, K., Wulf, A., and Ludwig, R. "Hydrogen Bonding in Protic Ionic Liquids: Reminiscent of Water," *Angewandte Chemie International Edition* Vol. 48, No. 17, 2009. doi: 10.1002/anie.200806224

[5] Berg, S. P. "Development of Ionic Liquid Multi-Mode Spacecraft Micropropulsion System," *Aerospace Engineering*. Vol. Doctoral, Missouri University of Science and Technology, Rolla, MO, 2015.

[6] Wainwright, M. J., Rovey, J.L., Miller, S., Prince, B.D., Berg, S.P. "Hydroxylammonium Nitrate Species in a Monopropellant Electrospray Plume," *Journal of Propulsion and Power*, 2019. doi: 10.2514/1.B37471

[7] Berg, S. P., Rovey, J. L., Prince, B., Miller, S., and Bemish, R. "Electrospray of an Energetic Ionic Liquid Monopropellant for Multi-Mode Micropropulsion Applications," *51st AIAA/SAE/ASEE Joint Propulsion Conference*. American Institute of Aeronautics and Astronautics, Orlando, FL., 2015. doi: 10.2514/6.2015-4011

[8] Miller, S. W., Prince, B. D., Bemish, R. J., and Rovey, J. L. "Mass Spectrometry of Selected Ionic Liquids in Capillary Electrospray at Nanoliter Volumetric Flow Rates," *52nd AIAA/SAE/ASEE Joint Propulsion Conference*. 2016. doi: 10.2514/6.2016-4740

[9] Prince, B. D., Fritz, B. A., and Chiu, Y.-H. "Ionic Liquids in Electrospray Propulsion Systems," *Ionic Liquids: Science and Applications*. Vol. 1117, American Chemical Society, 2012, pp. 27-49.

[10] Alonso-Matilla, R., Fernandez-Garcia, J., Congdon, H., Fernandez de la Mora, J. "Search for liquids electrospraying the smallest possible nanodrops in vacuo," *Journal of Applied Physics* Vol. 116, 2014. doi: 10.1063/1.4901635

[11] Berg, S. P., Rovey, J. L., and Wainwright, M. J. "Ignition of an Electrosprayable Monopropellant in a Submillimeter Catalytic Microtube," *JANNAF Propulsion Meeting*. 2018.

[12] Berg, S. P., and Rovey, J. L. "Assessment of Imidazole-Based Ionic Liquids as Dual-mode Spacecraft Propellants," *Journal of Propulsion and Power* Vol. 29, No. 2, 2013, pp. 339-351. doi: 10.2514/1.B34341

[13] Berg, S. P., and Rovey, J. L. "Decomposition of Double Salt Ionic Liquid Monopropellant in a Microtube for Multi-Mode Micropropulsion Applications," *53rd AIAA/SAE/ASEE Joint Propulsion Conference*. Atlanta, GA, 2017.
doi: 10.2514/6.2017-4755

[14] Berg, S. P., and Rovey, J. L. "Decomposition of Monopropellant Blends of Hydroxylammonium Nitrate and Imidazole-Based Ionic Liquid Fuels," *Journal of Propulsion and Power* Vol. 29, No. 1, 2013, pp. 125-135.
doi: 10.2514/1.b34584

[15] Donius, B. R., and Rovey, J. L. "Ionic Liquid Dual-Mode Spacecraft Propulsion Assessment," *Journal of Spacecraft and Rockets* Vol. 48, No. 1, 2011, pp. 110-123.
doi: 10.2514/1.49959

[16] Berg, S. P. a. R., J.L. "Assessment of Imidazole-Based Energetic Ionic Liquids as Dual-Mode Spacecraft Propellants," *Journal of Propulsion and Power* Vol. 29, No. 2, 2013, pp. 339-351.
doi: 10.2514/1.B34341

[17] Miller, S. W., Prince, B. D., Bemish, R. J., and Rovey, J. L. "Electrospray of 1-Butyl-3-Methylimidazolium Dicyanamide Under Variable Flow Rate Operations," *Journal of Propulsion and Power* Vol. 30, No. 6, 2014, pp. 1701-1710.
doi: 10.2514/1.B35170

[18] Wagaman, K. L. "Liquid monopropellant." The United States of America as represented by the Secretary of the Navy, The United States of America, 1999.

[19] Umebayashi, Y., Chung, W.L., Mitsugi, T., Fukuda, S., Takeuchi, M., Fujii, K., Takamuku, T., Kanzaki, R., and Ishiguro, S.I. "Liquid Structure and the Ion-Ion Interactions of Ethylammonium Nitrate Ionic Liquid Studied by Large Angle X-Ray Scattering and Molecular Dynamics Simulations," *Journal of Computer Chemistry, Japan* Vol. 7, No. 4, 2008, pp. 125-134.
doi: 10.2477/jccj.H2013

[20] Borrajo-Pelaez, R., Saiz, F., and Gamero-Castaño, M. "The Effect of the Molecular Mass on the Sputtering of Si, SiC, Ge, and GaAs by Electrosprayed Nanodroplets at Impact Velocities up to 17 km/s," *Aerosol Science and Technology* Vol. 49, 2015, pp. 256-266.
doi: 10.1080/02786826.2015.1023890

[21] Patrick, A. L., Vogelhuber, K. M., Prince, B. D., and Annesley, C. J. "Theoretical and Experimental Insights into the Dissociation of 2-Hydroxyethylhydrazinium Nitrate Clusters Formed via Electrospray," *Journal of Physical Chemistry A* Vol. 122, No. 8, 2018, pp. 1960-1966.
doi: 10.1021/acs.jpca.7b12072

[22] Steill, J. D., Szczepanski, J., and Oomens, J. "Structural characterization by infrared multiple photon dissociation spectroscopy of protonated gas-phase ions obtained by electrospray ionization of cysteine and dopamine," *Analytical and Bioanalytical Chemistry* Vol. 399, 2010, pp. 2463-2473.
doi: 10.1007/s00216-010-4582-y

[23] Zech, O., Thomaier, S., Kolodziejski, A., Touraud, D., Grillo, I. and Kunz, W. "Ethylammonium nitrate in high temperature stable microemulsions," *Journal of Colloid and Interface Science* Vol. 347, 2010, pp. 227-232.
doi: 10.1016/j.jcis.2010.03.031

[24] Ludwig, R. "A Simple Geometrical Explanation for the Occurrence of Specific Large Aggregated Ions in Some Protic Ionic Liquids," *Journal of Physical Chemistry B* Vol. 113, 2009, pp. 1541-15422.
doi: 10.1021/jp907204x

[25] Alavi, S., and Thompson, D. L. "Hydrogen Bonding and Proton Transfer in Small Hydroxylammonium Nitrate Clusters: A Theoretical Study," *The Journal of Chemical Physics* Vol. 119, No. 8, 2003, pp. 4274-4282.
doi: 10.1063/1.1593011

[26] Alavi, S. a. T., D.L. "Effects of Alkyl-Group Substitution on the Proton-Transfer Barriers in Ammonium and Hydroxylammonium Nitrate Salts," *The Journal of Physical Chemistry A* Vol. 108, No. 41, 2004, pp. 8801-8809.
doi: 10.1021/jp040189r

[27] Mohammed, O. F., Pines, D., Dreyer, J., Pines, E, and Nibbering, E.T.J. "Sequential Proton Transfer Through Water Bridges in Acid-Base Reactions," *Science* Vol. 3101, No. 5745, 2005, pp. 83-86.
doi: 10.1126/science.1117756

[28] Martins, V. L., Nicolau, B.G., Urahata, S.M., Ribeiro, M.C.C., and Torresi, R.M. "Influence of the Water Content on the Structure and Physicochemical Properties of an Ionic Liquid and Its Li+ Mixture," *Journal of Physical Chemistry B* Vol. 117, No. 29, 2013, pp. 8782-8792.
doi: 10.1021/jp312839z

[29] Wainwright, M. J., Miller, S., Prince, B.D., Berg, S.P., Rovey, J.L. "Mass Spectroscopy of a Multi-Mode Propellant in Anion and Cation Mode," *Join Propulsion Conference*. AIAA, Cincinnati, Ohio, 2018. doi: 10.2514/6.2.018-4725

[30] Kelkar, M. S., Shi, W., Maginn, E.J. "Determining the Accuracy of Classical Force Fields for Ionic Liquids: Atomistic Simulation of the Thermodynamic and Transport Properties of 1-Ethyl-3-methylimidazolium Ethylsulfate ([emim][EtSO4]) and Its Mixtures with Water," *Industrial & Engineering Chemistry Research* Vol. 47, No. 23, 2008, pp. 9115-9126. doi: 10.1021/ie800843u

[31] Ryan, C. N., Smith, K.L., Stark, J.P. "The Flow Rate Sensitivity to Voltage Across Four Electrospray Modes," *Applied Physics Letters* Vol. 104, 2014. doi: 10.1063/1.4866670

[32] Mair, G. L. R. "Theoretical Determination of Current-Voltage Curves for Liquid Metal Ion Sources," *Journal of Physics D: Applied Physics* Vol. 17, No. 11, 1984, p. 2323. doi: 10.1088/0022-3727/17/11/019

[33] Emel'yanenko, V. N., Boeck, G., Verevkin, S.P., and Ludwig, R. "Volatile Times fr the Very First Ionic Liquid: Understanding the Vapor Pressures and Enthalpies of Vaporization of Ethylammonium Nitrate," *Chemistry: A European Journal* Vol. 20, 2014, pp. 11640-11645. doi: 10.1002/chem.201403508

[34] Chiu, Y. H., Austin, B.L., Dressler, R.A., Levandier, D., Murray, P.T., Lozano, P., and Martinez-Sanchez, M. "Mass Spectrometric Analysis of Colloid Thruster Ion Emission from Selected Propellants," *Journal of Propulsion and Power* Vol. 21, No. 3, 2005, pp. 416-423. doi: 10.2514/1.9690

[35] Weingartner, H., Knocks, A., Schrader, W., and Kaatze, U. "Dielectric Spectroscopy of the Room Temperature Molten Salt Ethylammonium Nitrate," *Journal of Physical Chemistry A.* Vol. 105, 2001. doi: 10.1021/jp0114586

[36] Fernandez, A., Garcia, J, Torrecilla, J.S., Oliet, M., and Rodriguez, F. "Volumetric, Transport and Surface Properties of [bmim][MeSO4] and [emim][EtSO4] Ionic Liquids As a Function of Temperature," *Journal of Chemical & Engineering Data* Vol. 53, 2008. doi: 10.1021/je8000766

[37] Kennedy, D. F., and Drummond, C.J. "Large Aggregated Ions Found in Some Protic Ionic Liquids," *the Journal of Physical Chemistry B* Vol. 113, 2009, pp. 5690-5693. doi: 10.1021/jp900814y

[38] Chiu, Y. H., Gaeta, G., Levandier, D. J., Dressler, R. A., and Boatz, J. A. "Vacuum Electrospray Ionization Study of the Ionic Liquid, [Emim][Im]," *International Journal of Mass Spectrometry* Vol. 265, No. 2-3, 2007, pp. 146-158. doi: 10.1016/j.ijms.2007.02.010

[39] Ficke, L. E. R., H., Brennecke, J.F. "Heat Capacities and Excess Enthalpies of 1-Ethyl-3-methylimidazolium-Based Ionic Liquids and Water," *Journal of Chemical & Engineering Data* Vol. 53, 2008, pp. 2112-2119. doi: 10.1021/je800248w

[40] Politi, L., Morini, L., Groppi, A., Poloni, V., Pozzi, F., and Polettini, A. "Direct Determination of the Ethanol Metabolites Ethyl glucuronide and Ethyl Sulfate in Urine by Liquid Chromatography/ Electrospray Tandem Mass Spectrometry," *Rapid Communications in Mass Spectrometry* Vol. 19, 2005, pp. 1321-1331.
doi: 10.1002/rcm.1932

[41] de la Mora, J. F., and Loscertales, I. G. "The Current Emitted by Highly Conducting Taylor Cones," *Journal of Fluid Mechanics* Vol. 260, No. special issue, 1994, pp. 155-184. doi: 10.1017/S0022112094003472

[42] Huang, M. M., Jiang, Y,m Sasisanker, P., Driver, G.W., and Weingartner, H. "Static Relative Dielectric Permittivities of Ionic Liquids at 25°C," *Journal of Chemical & Engineering Data* Vol. 56, 2011, pp. 1494-1499.

[43] Heid, E., Docampo-A´lvarez, B., Varela, L.M., Prosenz, K, Steinhauser, O and Schröder, C. "Langevin behavior of the dielectric decrement in ionic liquid water mixtures," *Physical Chemistry Chemical Physics* Vol. 20, 2018, pp. 15106-15117.